Solid State Ionics 262 (2014) 230–233

Contents lists available at ScienceDirect

Solid State Ionics

journal homepage: www.elsevier.com/locate/ssi

Evaluation of aluminium doped lanthanum ferrite based electrodes for supercapacitor design

Atma Rai [a,*], A.L. Sharma [b], Awalendra K. Thakur [a,c]

[a] Department of Physics, Indian Institute of Technology, Patna, 800013, India
[b] Centre for Physical and Mathematical Sciences, Central University of Punjab, Bathinda, 151001, India
[c] Department of Physics and Meteorology, Indian Institute of Technology, Kharagpur, 721302, India

ARTICLE INFO

Article history:
Received 18 May 2013
Received in revised form 8 October 2013
Accepted 10 October 2013
Available online 6 November 2013

Keywords:
Supercapacitor
Cyclic voltammetry
EIS
Cycle
Cycle life

ABSTRACT

We report Al doped ferrites $La_{1-x}Al_xFeO_3$ ($x = 0, 0.3$) as an electrode material for supercapacitor design. The $La_{1-x}Al_xFeO_3$ has been synthesized via chemical route. Structural and microstructural evolution has been carried out by X-ray diffraction (XRD) analysis and field emission scanning electron microscopy (FESEM) respectively. The electrode property of $La_{1-x}Al_xFeO_3$ has been evaluated by using three electrode systems, glassy carbon (working), Pt (counter) and Ag/AgCl (reference electrode) with H_2SO_4 as the electrolyte. The Al doped ferrites show better cycle life (~250) and columbic efficiency (η) (~96%) in comparison to un-doped lanthanum ferrite sample. An increase in specific capacitance (~1.5 times) has also been observed in Al doped lanthanum ferrite in comparison to lanthanum ferrite. The maximum specific capacitance for Al doped lanthanum ferrite is ~260 F/g as compared to lanthanum ferrite ~200 F/g. The improved specific capacitance, columbic efficiency and cycle life of Al doped ferrites may be related to a relative decrease in equivalent series resistance (95 Ω for LFO to 55 Ω LAFO) and lower M.W. of Al doped lanthanum ferrite.

1. Introduction

At present, fossil fuels are the lifeline for automobiles including surface transport and other utilities. However, they are exhaustible. These sources have a limited lifetime and are polluting environment. So, search for an alternative energy source with features of high energy density, miniaturization and portability is much in demand. Supercapacitors are one such alternative with power storage capacity in the range 20–2000 F/g. Fuel cells, rechargeable batteries and electrolytic capacitors with high specific energy are some other examples of green and clean energy sources [1–10]. Amongst them, supercapacitors are the best alternatives because it offers power density higher than batteries and fuel cell and energy density higher than conventional capacitors. Based on the charge-storage mechanism supercapacitors are classified as; (i) electric double-layer capacitors (EDLC) with capacitive effect arising out of charge accumulation at the electrode electrolyte interface and, (ii) redox supercapacitors having pseudocapacitance, more than ten times greater than EDLC caused by superficial or multi-electron-transfer faradic reactions.

Electrodes with appropriate voltage stability, high surface area and good electronic conductivity play a very crucial role in supercapacitor performance. Multivalent transition metal oxides exhibit excellent pseudocapacitance. Literature reveals that RuO_2 based supercapacitors, though good in performance, suffer from high material cost, while amorphous MnO_2 based supercapacitors often exhibit poor cycle life. Another serious problem is its poor rate capability, i.e.; lack of sustainability at high discharge rate. In view of these difficulties, we aim to search performance with low cost alternative oxide, having layered structure with capability of fast redox reaction. Perovskite type functional oxides having structural and thermal stability are

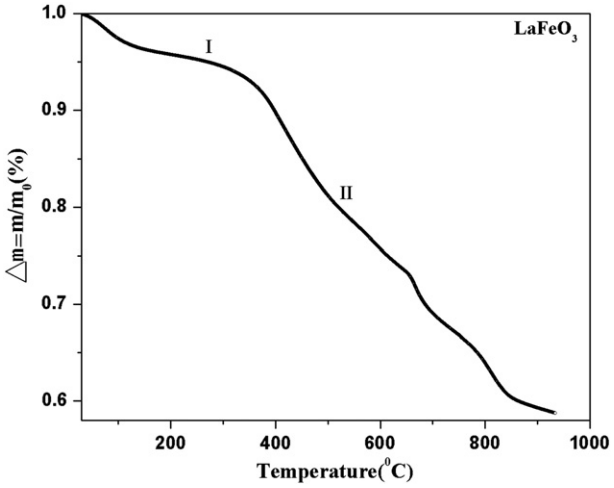

Fig. 1. Thermogravimetric analysis of lanthanum ferrite.

* Corresponding author.
E-mail address: atma@iitp.ac.in (A. Rai).

0167-2738/$ – see front matter © 2013 Elsevier B.V. All rights reserved.
http://dx.doi.org/10.1016/j.ssi.2013.10.024

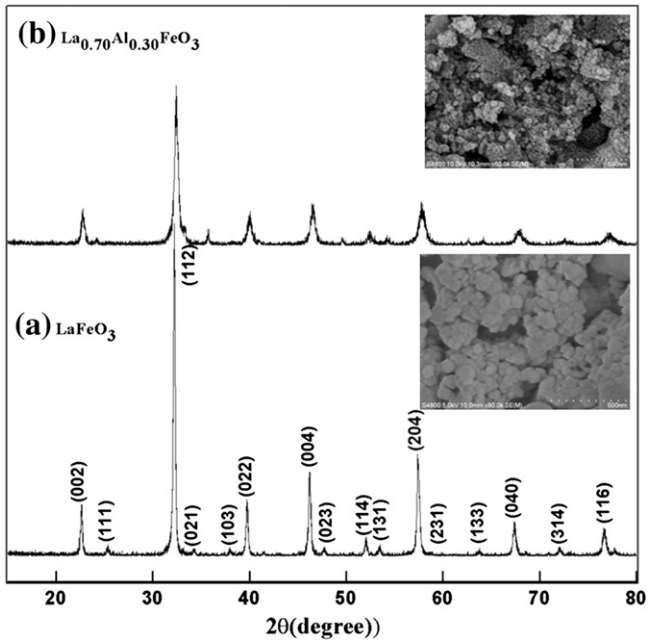

Fig. 2. XRD pattern of (a) $LaFeO_3$ and (b) $La_{0.7}Al_{0.3}FeO_3$ and FESEM micrograph (inset).

considered to be promising candidates for application as electrode in supercapacitor design.

Present paper reports electrode characteristics of Al based lanthanum ferrite ($La_{(1-x)}Al_xFeO_3$) for supercapacitor applications. The observed experimental results are likely to open a new window of low cost metal oxide with high rate capability and improved electrochemical performance vis-a-vis earlier reports on electrodes [11–19].

2. Experimental procedure

The citrate–nitrate auto ignition method was adopted for the preparation of lanthanum aluminium ferrite (LAFO) powder. Calculated amount of acetates of lanthanum and aluminium and nitrates of iron was disolved into a small amount of distilled water. The homogeniously mixed solution turned into a gel during heating. The air-dried powder of the parent compound ($LaFeO_3$ and $La_{(1-x)}Al_xFeO_3$) was calcined at an optimized temperature ~850 °C for two hours based on prior optimization using thermogravimetric analysis (TGA) technique. The phase identification/formation of all the prepared ferrite samples was carried out by an X-ray powder diffractometer (model: RIGAKU-TTRAX3) with CuKα radiation (λ = 1.5418 Å) over a wide range of Bragg's angles (2θ) ($10° \le 2\theta \le 80°$) at a resolution of 0.01°. No secondary or impurity phase has been found within error limit of XRD. Field emission scanning electron microscope (FESEM) (model: HITACHI-54800) was employed to record the surface morphology of the sample. Electrochemical measurments were performed on a supercapacitor cell designed using a three electrode cell comprising of glassy carbon (working), platinum (counter) and Ag/AgCl(reference) electrodes. The sample powder was mounted on glassy carbon using NMP as binder and H_2SO_4(1 M) as an electrolyte. Supercapacitor performance has been evaluated using CH Instruments (model: CHI 760D). Specific Capacitance (C_s) has been estimated using the relation;

$$C_s = I \times \frac{dt}{dV} \Big/ \frac{Q}{F}\frac{M}{z} \quad (1)$$

I = Current, dv/dt = Slope of charge–discharge curve, Q = Charge, M = molecular weight, F = Faraday constant, z = Electrons transferred per ion.

3. Results and discussion

3.1. Thermogravimetric analysis

Fig. 1 shows the thermogravimetric analysis (TGA) pattern of $LaFeO_3$ (LFO) sample. The thermogram shows two distinct regions of mass loss as marked in Fig. 1. The region I of mass loss begin at 100 °C and it continues at a steady rate up to ~350 °C. It is followed by a steep loss marked as region II suggesting progressive mass loss ($\Delta m/m_0$) with rise in temperature. The gradual loss (region I) up to 350 °C may be due to the loss of surface adsorbed moisture during thermal decomposition of precursor compounds. The progressive mass loss (step loss marked as region II) up to ~800 °C might be assigned to the thermal oxidative degradation. Beyond 800 °C, mass loss becomes stable. The formation temperature of LFO may be ≥800 °C. So, based on this optimization; sample calcination was carried at 850 °C for two hours.

3.2. Structural and microstructural analysis

Fig. 2 shows the X-ray diffraction pattern of aluminum doped lanthanum ferrites, $La_{1-x}Al_xFeO_3$ (where x = 0, and 0.30) samples. The XRD peaks were indexed as per ICDD file and the lattice parameters were determined in the orthorhombic crystal system using well known Full Prof software. It can be seen from the Fig. 2(a) and (b) that the Al doped lanthanum ferrite ($La_{(1-x)}Al_xFeO_3$) shows identical peaks like $LaFeO_3$ and main peak has been indexed as [112]. The peak pattern suggests significant degree of polycrystallinity. The lattice constants of lanthanum ferrites are estimated as; a = 5.5587 Å, b = 7.8639 Å, c = 5.5484 Å, α = β = γ = 90° respectively. In addition, the crystallite size is calculated to be ~38 nm by fitting most intense peak and using Scherrer formula. XRD pattern indicated single phase LFO with orthorhombic crystal structure and Pnma (62) space group. The structural parameters are given in the Table 1.

The surface morphology of $La_{1-x}Al_xFeO_3$ (x = 0, and 0.30) is shown in inset of Fig. 2. It is noted that the polycrystalline LFO and LAFO particles (average sizes 40 nm) are uniformly distributed. The smaller particle size of ferrites under study, which is an outcome of the sample processing method, is expected to have larger specific surface area and shorter diffusion pathway for ion migration. For the active material, the smaller particles have larger effective surface area and shorter diffusion distance, which can provide faster mobility, higher material utilization, and improved rate performance.

3.3. Electrochemical analysis

Electrode characteristics of this rare earth based Al doped ferrite have been evaluated with a three electrode system comprising of glassy carbon (working), Ag/AgCl (reference) and Pt (counter) electrode and

Table 1
A comparative structural parameters of $LaFeO_3$ and $La_{0.7}Al_{0.3}FeO_3$.

System	Crystal structure	a (Å)	b (Å)	c (Å)	α = β = γ (degree)	V $(Å)^3$	Tolerance factor(t)
$LaFeO_3$	Orthorhombic	5.5587	7.8639	5.5484	90	242.5	0.906
$La_{0.7}Al_{0.3}FeO_3$	Orthorhombic	5.5065	7.8031	5.5514	90	238.5	0.835

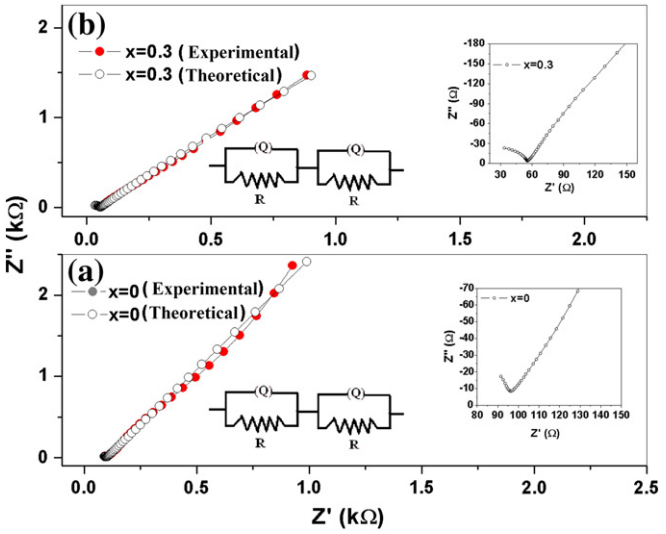

Fig. 3. Electrochemical impedance (EIS) pattern of (a) $LaFeO_3$ and (b) $La_{0.7}Al_{0.3}FeO_3$.

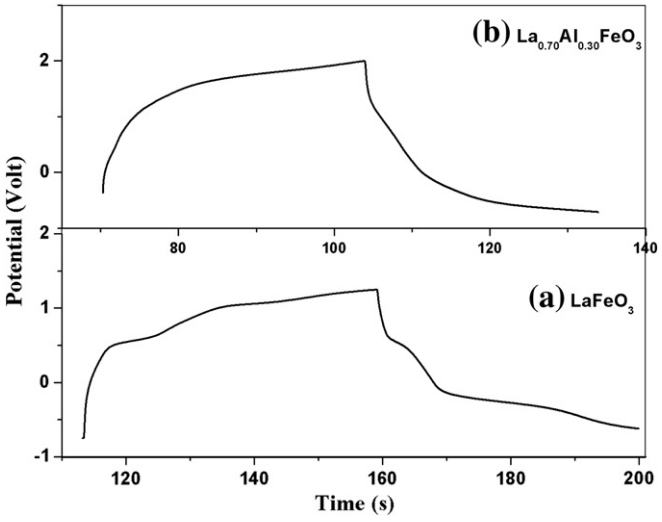

Fig. 5. Charge–discharge profile of (a) $LaFeO_3$ and (b) $La_{0.7}Al_{0.3}FeO_3$.

aq. H_2SO_4 (1 M) as the electrolyte. The electrochemical impedance spectroscopy measurement was performed to evaluate charge transfer during charging and discharging cycle. The electrochemical impedance spectroscopy (EIS) profile (Fig. 3) gives a typical response comprising of a small high frequency arc followed by a low frequency spike. The bulk resistance (R_b) of the sample has been estimated using the intercept of the higher frequency arc on real axis. The experimental impedance data has been fitted using non-linear least squares (NLS) model by means of a computer program Z_{Simp}Win. An equivalent electrical circuit model based on theoretical analysis agrees well with the experimental results of impedance spectrum. It is shown for comparison in the inset of Fig. 3. It comprises of parallel combination of resistance (R) and the constant phase element (cpe) connected in series with another parallel combination of resistance (R) and the constant phase element (cpe). The high frequency arc suggests conducting property whereas low frequency step spike is attributed to the capacitive response due to charge transfer reaction.

Cyclic voltammogram (Fig. 4(a, b)) is recorded in the potential window of −1.5 to 1.5 V for LFO and −1 to +2 V for LAFO at a scan rate of 0.5 V/s. Anodic peaks (0.33 V) occur due to oxidation during discharge and cathodic peak (0.58 V) is due to reduction. It may be related to the formation of redox couple Fe^{+2}/Fe^{+3} and Fe^{+3}/Fe^{+2} respectively during charge transfer reaction [13,15]. The stability of cyclic performance has been evaluated over a large number of cycles at different scan rates. Calculations indicate that the specific capacitance of LAFO sample is nearly 1.5 times higher when compared with the LFO sample. The proposed reaction mechanism for LFO and LAFO is given as; $LaFeO_3 + xH^+ + xe^- = LaFeO_{3-x}(OH)_x$ and $La_{0.7}Al_{0.3}FeO_3 + xH^+ + xe^- = La_{0.7}Al_{0.3}FeO_{3-x}(OH)_x$ respectively.

The charge–discharge performance of the supercapacitor cell was evaluated in the potential window of 2 V for the LFO and LAFO samples under study. The charge–discharge plot (Fig. 5) shows a marked deviation from the ideal capacitor response due to the presence of internal resistance in the electrode material. The observation agrees well with the EIS results discussed earlier. The estimated equivalent series resistance (ESR) is ~95Ω & 55Ω for LFO and LAFO respectively.

The Coulombic efficiency (η) of the capacitor cell has been calculated from the galvanostatic charge–discharge experiments as follows:

$$\eta(\%) = \frac{\nabla t_D}{\nabla t_C} \times 100 \quad (2)$$

where, Δt_D and Δt_C discharging and charging times respectively with the same current [20]. Based on calculations, it is found that the coulombic efficiency of LAFO sample is 96% which is 15% higher (Fig. 6b) when compared with LFO sample (Fig. 6a).

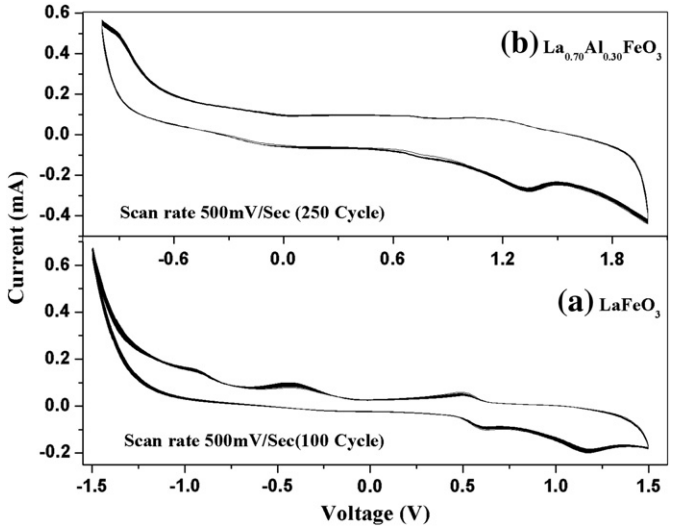

Fig. 4. Cyclic voltammogram of (a) $LaFeO_3$ and (b) $La_{0.7}Al_{0.3}FeO_3$ with scan rate 500 mV/s.

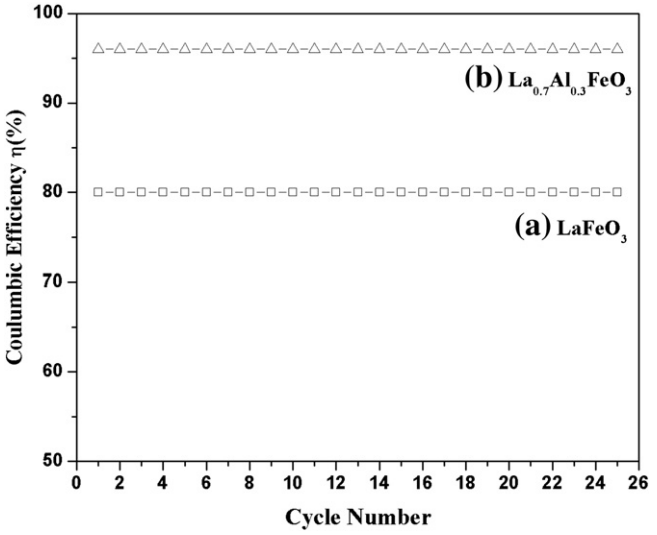

Fig. 6. Coulombic efficiency of (a) $LaFeO_3$ and (b) $La_{0.7}Al_{0.3}FeO_3$.

4. Conclusions

Perovskite type ferrites have been investigated for their suitability as electrode for supercapacitor application. Effect of Al doping in $LaFeO_3$ has shown large enhancement in storage capacity with significant improvement in columbic efficiency. A very stable cycle life has also been noted. It is concluded that Al doped lanthanum ferrite $La_{0.7}Al_{0.3}FeO_3$ may be a good electrode material for supercapacitor design with high rate capability.

References

[1] S.A. Hashmi, A. Kumar, S.K. Tripathi, Eur. Polym. J. 41 (2005) 1373.
[2] S.C. Pang, M.A. Anderson, T.W. Chapman, J. Electrochem. Soc. 147 (2000) 444.
[3] L. Permann, M. Latt, J. Leis, M. Arulepp, Electrochim. Acta 51 (2006) 1274.
[4] B.E. Conway, Electrochemical Supercapacitors, Plenum Publishing, New York, 1999.
[5] Hu. Chi-Chang, Ta-Wang Tsou, J. Power Sources 115 (2003) 179.
[6] F. Lufrano, P. Staiti, Int. J. Electrochem. Sci. 5 (2010) 903.
[7] Hong-Ying Wu, Huan-Wen Wang, Int. J. Electrochem. Sci. 7 (2012) 4405.
[8] S. Ravi, V.S. Prabhin, Adv. Mater. Lett. 4 (2013) 296.
[9] H. Xia, Y.S.M.G. Yuan, C. Cui, L. Lu, Electrochem. Solid-State Lett. 15 (2012) A60.
[10] V. Srinivasan, W. John, J. Power Sources 108 (2002) 15.
[11] M.A. Arillo, M.L. Lopez, C. Pico, M.L. Veiga, Chem. Mater. 17 (2005) 4162.
[12] M. Krause, K. Knese, P. Wartewig, H. Langbein, Hyperfine Interact. 94 (1994) 1839.
[13] S.-L. Kuo, N.-L. Wu, Electrochem. Solid State Lett. 8 (2005) A495.
[14] M.A. Arillo, M.L. Lopez, E. Perez-Cappe, C. Pico, M.L. Veiga, Solid State Ionics 107 (1998) 307.
[15] S.-L. Kuo, N.-L. Wu, J. Power Sources 162 (2006) 1437.
[16] A.V. Rosario, L.O.S. Bulhoes, E.C. Pereira, J. Power Sources 158 (2006) 795.
[17] Y.R. Ahn, C.R. Park, S.M. Jo, D.Y. Kim, Appl. Phys. Lett. 90 (2007) 122106.
[18] T.C. Girija, M.V. Sangaranarayanan, J. Power Sources 156 (2006) 705.
[19] M.D. Stollar, R.S. Ruoff, Energy Environ. Sci. 3 (2010) 1294.
[20] Z.A. Hu, Y.L. Xie, Y.X. Wang, H.Y. Wu, Y.Y. Yang, Z.Y. Zhang, Electrochim. Acta 54 (2009) 2737.